SIMULIA Living Heart Human Model

Documentation

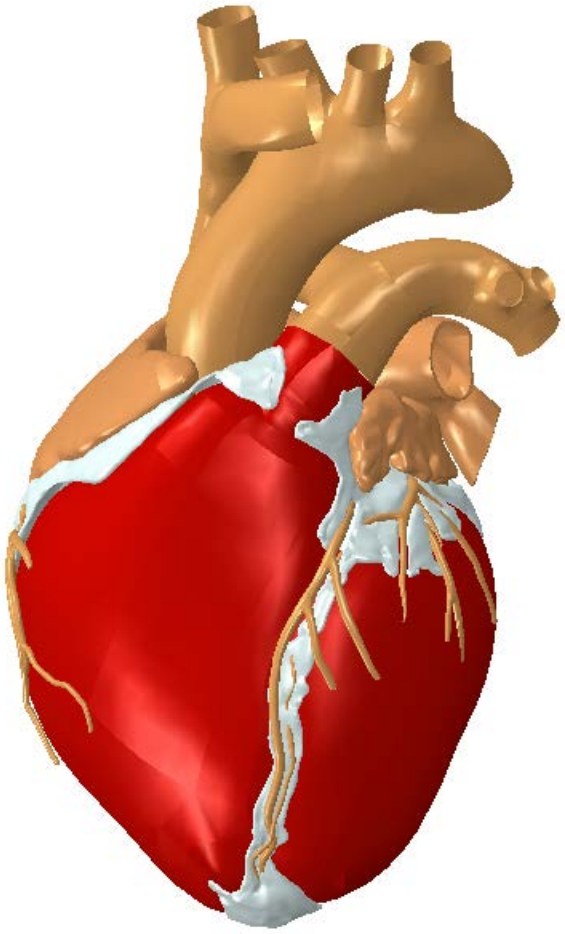

Abaqus 6.14

Legal Notices

Contents

1 About the Heart Model

The SIMULIA Living Heart Human Model (hereafter referred to as the "Heart Model") is a dynamic high-fidelity model of a normal (healthy), 4-chamber adult male human heart. It includes well-defined anatomic details of the heart as well as proximal vasculature, such as the aortic arch, pulmonary artery, and superior vena cava (SVC). The dynamic response of the Heart Model is governed by realistic electrical, structural, and fluid (blood) flow physics. As such, it can be used to study the electrical behavior of the heart by itself or to examine its coupled electromechanical behavior wherein the mechanical response is driven by an electrical excitation. Although the Heart Model represents a healthy heart, you can also study abnormal (diseased) states by modifying any of its geometry, material properties, and/or loads and boundary conditions. In addition, you can introduce other parts into the model (such as medical devices) to study their influence on cardiac function and explore treatment options.

The Heart Model includes the definition of a sequentially coupled electrical-mechanical analysis of a beat cycle with a one-second duration, which corresponds to a heart rate of 60 beats per minute, a typical adult (resting) heart rate. The electrical analysis is conducted in Abaqus/Standard for a single beat cycle. The mechanical analysis is conducted in Abaqus/Explicit for three beat cycles to reach a steady state and largely eliminate initial transient effects.

Sections 4 through 10 of this document discuss the Heart Model geometry, material properties, loads, boundary conditions, and analyses definitions. Section 11 presents a series of results, including some that are clinically meaningful. You can use Abaqus/CAE to examine and modify the model attributes and view additional outputs more relevant to your particular applications. Lastly, Section 12 discusses model verification and validation.

2 Units

The heart electrical model uses a consistent set of units as shown in **Table 2.0.1**.

Table 2.0.1: Electrical Model Units

Quantity	Units
Length	millimeter (mm)
Time	milliseconds (ms)
Voltage	millivolt (mV)
Conduction parameter	(mm^2/ms)

The heart structural model uses a consistent set of units as shown in **Table 2.0.2**.

Table 2.0.2: Mechanical Model Units

Quantity	Units
Mass	tonne (t)
Length	millimeter (mm)
Time	seconds (s)
Force	Newton (N)
Moment	Newton-millimeter (N-mm)
Stress	Megapascal (MPa)

3 Version Information

The Heart Model has been developed and tested with **Abaqus 6.14-3**. It is expected that the model will work with any maintenance release of Abaqus later than 6.14-3. The Heart Model is **not compatible** with any release of Abaqus prior to 6.14-3.

4 Heart Model Geometry

The NURBS geometry for the heart (at 70% ventricular diastole) comprises an assembly of individual parts. Most parts are meshed and included in the analyses. However, some parts are meshed and not included in the analysis while other parts are not meshed. These additional parts are made available and can be incorporated in other applications if needed. Other than the bundle of His and Purkinje fibers, all of the geometry was supplied by Zygote Media Group, Inc., although some of the original parts were modified to enhance mesh discretization.

Table 4.0.1 lists the geometric attributes for both the NURBS and discretized geometric representations. Some parts are used in either the electrical or mechanical analyses; some are used in both analyses, while some are not used in either analysis. Discretized parts used in both the electrical and mechanical simulations possess the same mesh topology. The subsections that follow provide additional detail on the modeling approaches used for various parts of the cardiac anatomy.

Table 4.0.1: Summary of Heart Model geometric attributes

Part Name	Description	Dimensionality	Element Type	Simulation Usage	Elements
Aortic_Arch	Aortic Arch	Surface	S4R, SFM3D3	Mechanical	1777
Aortic_Valve	Aortic Valve	Solid	None	Not used	--
Chordae_Tendineae	Chordae Tendineae	Line	T3D2	Not used	1135
Compliance	Three fluid chambers to incorporate the compliance of the arterial, venous, and pulmonary systems.	Surface	SFM3D4R	Mechanical	6
Coronary_Arteries1	Left Coronary Arteries	Surface	S4R	Not used	8194
Coronary_Arteries2	Right Coronary Arteries	Surface	None	Not used	--
Coronary_Sinus_Valve	Valve of the Coronary Sinus	Solid	None	Not used	--
Coronary_Veins1	Left Coronary Veins	Surface	None	Not used	--
Coronary_Veins2	Right Coronary Veins	Surface	None	Not used	--
Fat	Cardiac Fat	Solid	C3D4	Not used	54131
Fiber_Bundles	The electrical representation of the bundle of His and Purkinje network	Line	DC1D2	Electrical	654
Fossa_Ovalis	Fossa Ovalis	Solid	C3D4	Not used	354
L_Atrium	Left Atrium	Solid, Surface	DC3D4, C3D4, SFM3D3	Electrical, Mechanical	45430
Mitral_Valve	Mitral Valve	Solid	None	Not used	--
Pulmonary_Trunk	Pulmonary Trunk	Surface	S4R, SFM3D3	Mechanical	1425
Pulmonary_Valve	Pulmonary Valve	Surface	None	Not used	--
R_Atrium	Right Atrium	Solid, Surface	DC3D4, C3D4, SFM3D3	Electrical, Mechanical	62574
Superior_Vena_Cava	Superior Vena Cava	Surface	S4R, SFM3D3	Mechanical	1287
Tricuspid_Valve	Tricuspid Valve	Solid	None	Not used	--
Vena_Cava_Valve	Valve of the Vena Cava	Solid	None	Not used	--
Ventricles	Left and right ventricles.	Solid, Surface	DC3D4, C3D4, SFM3D3	Electrical, Mechanical	262972

4.1 Spatial Orientation of the Heart

The global orientation for the model within the model database is summarized in **Figure 4.1.1**. The owner of the heart is facing the +z direction.

Abaqus Orientation	Body Plane
X-Y Plane	Coronal
Y-Z Plane	Sagittal
Z-X Plane	Transverse

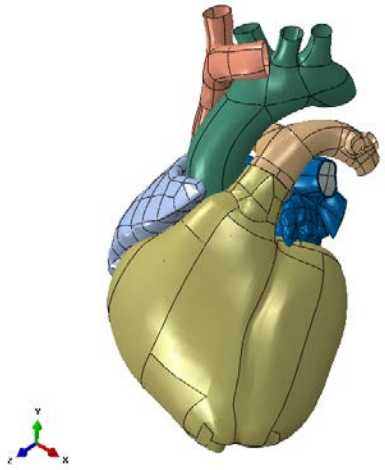

Figure 4.1.1: Spatial orientation of the heart

4.2 The Bundle of His and Purkinje Fibers

Representative geometry for the bundle of His and Purkinje fibers was approximated using the methodology described in **Kotikanyadanam et al. [1]**, where these structures are modeled as 1D electrical conduction elements (DC1D2) with higher conduction velocity than the surrounding cardiac tissue. The DC1D2 elements were created on the endocardial surface of the ventricles. The fiber elements are shown in **Figure 4.2.1**.

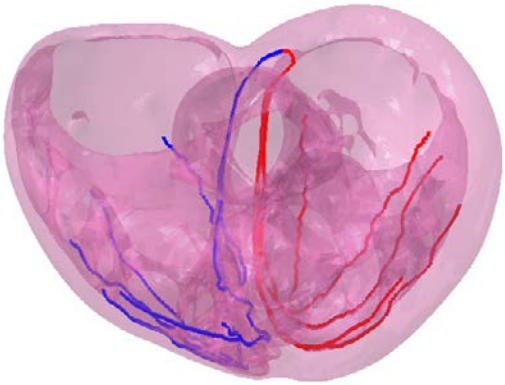

Figure 4.2.1: The Bundle of His and Purkinje fiber elements (Red: Left branch, Blue: Right branch)

4.3 Coronary Arteries and Veins

The major coronary arteries and veins (both on the left and right side of the heart) are included in the model, although they are not used in the simulation. The left coronary artery tree is shown in **Figure 4.3.1**. To include these parts in the mechanical analysis:

1. Mesh the geometry using a suitable technique (e.g., shells or solids).
2. Assign suitable material models (e.g., isotropic/anisotropic hyperelastic) and section definitions. Wherever an anisotropic material model is used, an orientation must also be assigned.
3. Instance and position the coronary arteries/veins appropriately.
4. Couple the base (see **Figure 4.3.1**) of the coronary tree to aorta. This can be done with a **Shell-to-Solid Coupling**. Repeat the process for the coronary vein by connecting it to the inferior vena cava.
5. Create a **Tie Constraint** between the remaining mating surfaces of the coronary artery/vein tree and the ventricles.

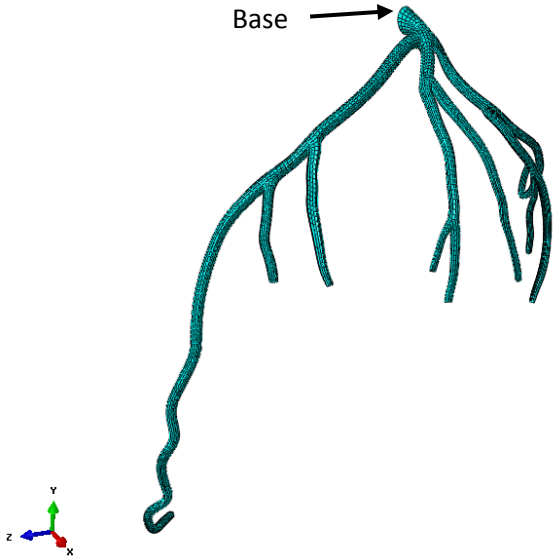

Figure 4.3.1: Mesh for the left coronary artery tree

4.4 Heart Valves

The NURBS geometry of the valves (tricuspid, mitral, pulmonary, and aortic) is included in the Heart Model but is not used in the simulation. Instead, simple planar surfaces representing the valves were created and meshed and demarcate the atrioventricular boundaries and the boundaries between the ventricles and the aorta and pulmonary trunk (as shown in **Figure 4.4.1**). This simplification is consistent with the hydrostatic fluid cavity approach (see Section 7) used to model blood flow between the chambers and in/out of the heart. If you need to model the valves (or blood flow) with greater fidelity, you can replace the planar surfaces with the true valve geometry, assign them either a solid or shell section, and connect them to the ventricles using **Tie Constraints** or **Shell-to-Solid Couplings**, respectively. **Baillargeon et al. [2]** used this approach to study mitral valve regurgitation.

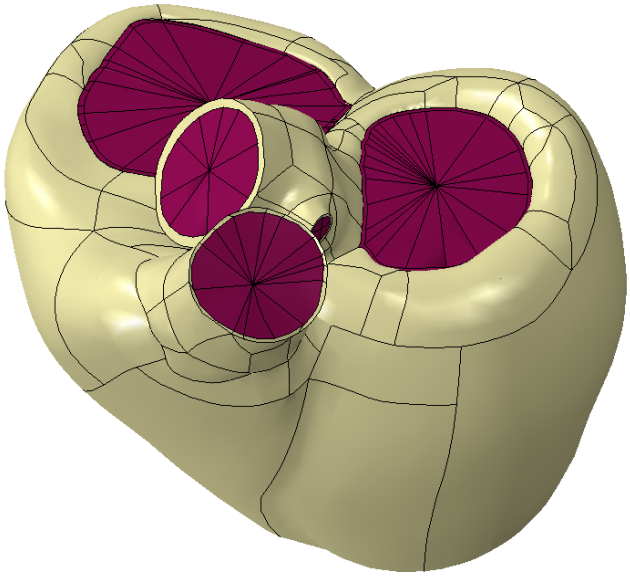

Figure 4.4.1: Planar surfaces (shown in magenta) representing the four heart valves

4.5 Chordae Tendineae

The chordae tendineae geometry is included in the Heart Model but is not used in the analyses due to the approach used to model the heart valves (See Section 4.4). However, the chordae have been meshed with truss elements (T3D2) as shown in **Figure 4.5.1** for your convenience. If the chordae are needed, they can be coupled to the ventricular papillary muscles and mitral/tricuspid valves via **Distributing Coupling** constraints. The methodology is similar to that used by **Prot et al. [3]**.

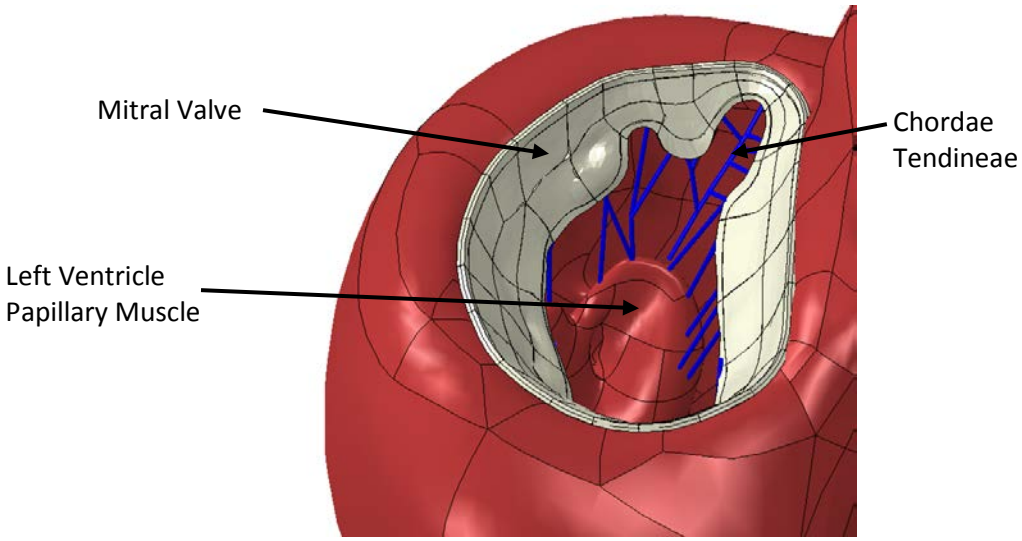

Figure 4.5.1: Chordae tendineae in the left ventricle modeled as truss elements

5 Material Properties

The values of the material constants used in the passive, active, and electrical constitutive laws discussed in the following subsections were initially set to those in the cited references; however, several values were modified during the model validation process to obtain quantitatively realistic (i.e., physiologically observed) behavior. The modified values are encrypted; however, you can override any of the values using the instructions provided in the **Question & Answer** article entitled "***Changing Parameter Values in the SIMULIA Living Heart Human Model***" accessible from the Knowledge Base. Furthermore, the material behavior of any region of the model can be entirely replaced with (i) any of the Abaqus built-in constitutive laws, or (ii) your own constitutive laws defined via user subroutines. Details on both approaches can be found in Chapters 21-26 of the **Abaqus Analysis User's Guide [4].**

5.1 Passive Tissue Response

The passive material response of the cardiac tissue uses an anisotropic hyperelastic formulation based on that proposed by **Holzapfel and Ogden [5]**. The deviatoric response is governed by the following strain energy potential with parameters as defined in **Table 5.1.1**,

$$\Psi_{dev} = \frac{a}{2b} exp[b(I_1 - 3)] + \sum_{i=f,s} \frac{a_i}{2b_i} \{exp[b_i((I_{4i} - 1)^2)] - 1\} + \frac{a_{fs}}{2b_{fs}} \left[exp\left(b_{fs} I_{8fs}^2\right) - 1\right],$$

Table 5.1.1: Holzapfel Deviatoric Parameters

Parameters	Description
a, b	Governs the isotropic response of the tissue
a_f, b_f	Governs the additional stiffness in the fiber direction
a_s, b_s	Governs the additional stiffness in the sheet direction
a_{fs}, b_{fs}	Governs the coupling stiffness in the f- and s-directions
I_1	The first deviatoric strain invariant
I_{4i}	A pseudo-invariant defined as $A_i \cdot C \cdot A_i$
I_{8fs}	A pseudo-invariant defined as $A_f \cdot C \cdot A_s$
C	Right Cauchy-Green deformation tensor
A_i	Vector in direction i

while the volumetric response is governed by

$$\Psi_{vol} = \frac{1}{D}\left(\frac{(J^2 - 1)}{2} - ln(J)\right),$$

with parameters as defined in **Table 5.1.2**.

Table 5.1.2: Holzapfel Volumetric Parameters

Parameters	Description
D	Multiple of bulk modulus ($K = 2/D$)
J	The third deformation gradient invariant

The values of the parameters are calibrated such that the myocardial strains predicted by the simulation compare favorably to those experimentally measured by **Genet et al. [6]** (see **Figure 5.1.1**). Note that since Genet et al. assumed a transversely isotropic response, the material response of the sheet and normal directions is identical.

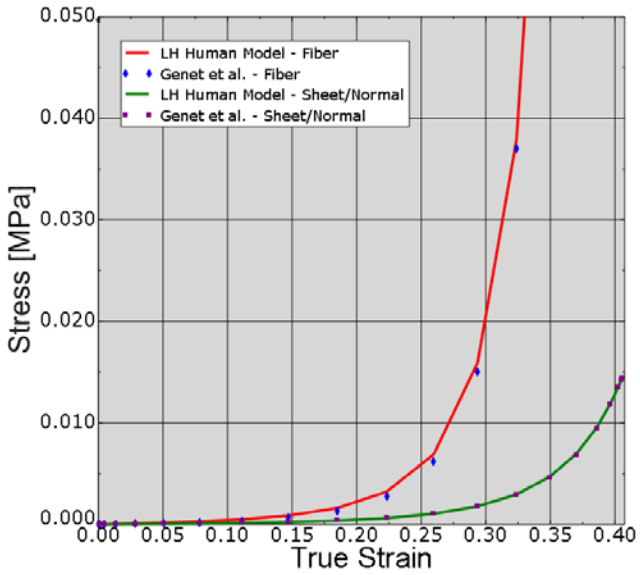

Figure 5.1.1: Comparison of passive material response between Genet et al. and the Heart Model

5.2 Active Tissue Response

The active tissue response (intended to capture the Frank-Starling effect) affects the stress components in the fiber and sheet directions in the constitutive model. Therefore, the total stress in the fiber direction, σ_f, is equal to the active stress, σ_{af}, plus the passive stress, σ_{pf}:

$$\sigma_f = \sigma_{pf} + \sigma_{af}$$

The active stress in the cardiac muscle fiber direction is defined by the following time varying elastance model (**Walker et al [7]**):

$$\sigma_{af}(t, E_{ff}) = \frac{T_{max}}{2} \frac{Ca_0^2}{Ca_0^2 + ECa_{50}^2(E_{ff})} \left(1 - cos\left(\omega(t, E_{ff})\right)\right),$$

where

$$ECa_{50}(E_{ff}) = \frac{Ca_{0_{max}}}{\sqrt{e^{B(l(E_{ff}) - l_0)} - 1}}$$

$$\omega(t, E_{ff}) = \begin{cases} \pi \dfrac{t}{t_0} when\ 0 \le t \le t_0 \\ \pi \dfrac{t - t_0 + t_r\left(l(E_{ff})\right)}{t_r} when\ t_0 \le t \le t_0 + t_r\left(l(E_{ff})\right) \\ 0\ when\ t \ge t_0 + t_r\left(l(E_{ff})\right) \end{cases}$$

$$t_r(l) = ml + b$$

$$l(E_{ff}) = l_r\sqrt{2E_{ff}+1}$$

with parameters as defined in **Table 5.2.1**.

Table 5.2.1: Constitutive parameters for the active tissue response

Parameters	Description
T_{max}	Constitutive law contractility scaling factor (value directly scales ejection fraction)
Ca_0	The peak intercellular calcium concentration
$Ca_{0_{max}}$	The maximum intercellular calcium concentration
B	Governs the shape of peak isometric tension-sarcomere length relation
l_0	The sarcomere length below which no active force develops
t_0	Time to reach the peak tension
m, b	Coefficients that govern the shape of the linear relaxation duration and sarcomere length relaxation
E_{ff}	Lagrangian strain tensor component aligned with the local muscle fiber direction
l_r	The initial sarcomere length

Active stress in the sheet direction, σ_s, is the sum of the passive stress, σ_{ps}, and a fraction of the stress in the fiber direction, $n * \sigma_{af}$ (where *n* is a scalar value less than 1.0 and represents the interaction between the adjacent muscle fibers):

$$\sigma_s = \sigma_{ps} + n * \sigma_{af}$$

The value of *n* affects not only the total contractility of the chambers, but also the degree of twist developed in the chamber during the cardiac cycle. The magnitude of contractility for each chamber was tuned to provide the appropriate ejection fraction for that chamber. This involved the tuning of T_{max}, *n* (to limit the twist of the LV and RV), and l_0.

5.3 Viscoelasticity

Isotropic time dependent linear viscoelasticity is defined as part of the material constitutive behavior (see Section 22.7.1 "Time domain viscoelasticity" in the **Abaqus Analysis User's Guide [4]**) to damp out the high frequency response during ventricular systole (contraction). While cardiac tissue is generally known to exhibit viscoelastic behavior, suitable experimental data on cardiac viscoelasticity were not available; hence, the Heart Model incorporates a small amount of viscoelasticity to eliminate unrealistic transient behavior.

5.4 Tissue Electrical Response

The electrical response of the tissue is characterized by an action potential, ϕ, and recovery variable, *r,* (**Hurtado and Kuhl [8]**). The global electrical analysis assumes a monodomain response:

$$\dot{\phi} + div(q(\phi)) = f^{\phi}(\phi, r),$$

where the flux term, *q,* characterizes the propagating nature of the electrical waves:

$$q = -D\nabla\phi.$$

The term, *D,* is a second-order diffusion tensor, which can account for anisotropic diffusion.

The source term, f^{ϕ}, characterizes the local action potential profile:

$$f^{\phi}(\phi, r) = c\phi[\phi - \alpha][1 - \phi] - r\phi$$

The local biochemical portion of the analysis is modeled through a temporal evolution of the recovery variable, *r:*

$$\dot{r} = f^{r}(\phi, r)$$

The source term, f^{r}, characterizes the slow features of the action potential:

$$f^{r}(\phi, r) = [\gamma + r\bar{\gamma}(\phi)]\big[-r - c\phi[\phi - b - 1]\big],$$

where

$$\bar{\gamma}(\phi) = \frac{\mu_1}{\mu_2 + \phi}$$

with parameters as defined in **Table 5.4.1**.

Table 5.4.1: Constitutive Parameters for the electrical response

Parameters	Description
c	Scaling parameter for the source term, f^{ϕ}
α	Oscillation threshold (positive values characterize stable non-pacemaker cells, negative values characterize oscillatory pacemaker cells)
γ	Refractoriness that governs the time it takes the tissue to repolarize (i.e., time to get back to the resting potential)
b	A phenomenological scaling parameter
μ_1, μ_2	Scaling factors that control the shape of the restitution curve

The electrical properties are calibrated to provide physiologically observed activation times (See **Conduction Systems Tutorial [9]**). The bundle of His and Purkinje fibers are assigned conduction parameters that generate the physically observed wave propagation pattern within the heart whereby the electrical signal first travels down the ventricular septum to the apex and then up the ventricular side walls.

6 Cardiac Tissue Fiber Orientations

The anisotropy of cardiac tissue requires a local orientation definition to be assigned to the elements in the model. As shown in **Figure 6.0.1**, the fiber orientations associated with the structures in the heart are complex due to:

- The complex organic geometry of the heart
- Orientations changing across the surface of the heart
- Orientations changing through the thickness of the heart wall

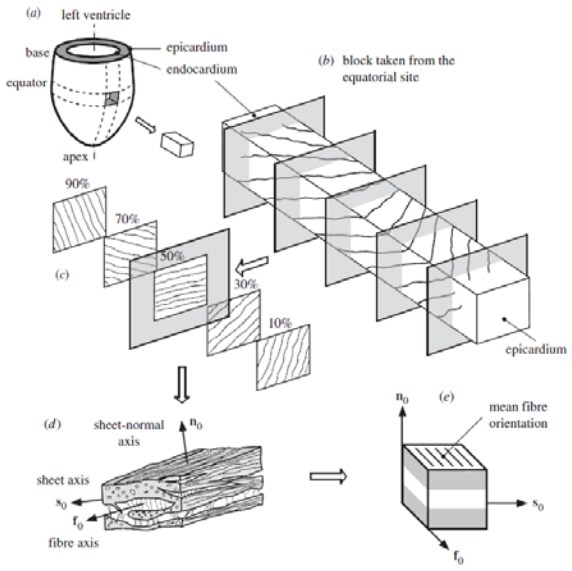

Figure 6.0.1: Schematic representation of muscle fiber orientation within the left ventricle (Holzapfel and Ogden [5])

For the atria and ventricles, local material orientations are defined as a **Discrete Field** in Abaqus/CAE. This methodology requires that a separate orientation be defined at the centroid of each element. The fiber angles, α, in the ventricles are approximately equal to -60° on the epicardium and +60° on the endocardium as shown in **Figure 6.0.2** taken from **Streeter et al. [10]**, which is consistent with **Genet et al. [6]**. As shown in **Figure 6.0.3**, the fiber orientations in the atria (as well as the superior vena cava, aortic arch, and pulmonary trunk) were approximated using Figure 20 in the **euHeart Final Project Report** **[11]**. The model includes three **Discrete Field** definitions (named **`R_Atrium`**, **`L_Atrium`**, and **`Ventricles`**).

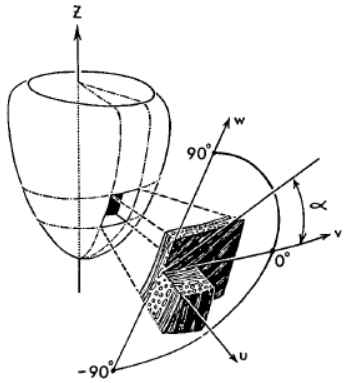

Figure 6.0.2: Definition of Helical Angle, α (taken from Streeter et al [10]).

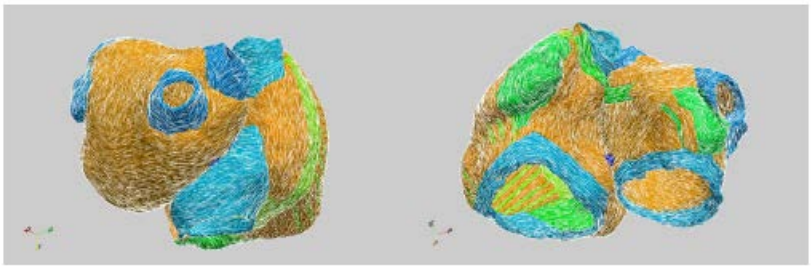

Figure 6.0.3: Fiber Orientations in the atrium (taken from Figure 20 of euHeart Final Project Report [11])

For the SVC, aortic arch, and pulmonary trunk, local material orientations are defined using the part geometry instead of a **Discrete Field**, since they are essentially tubular surfaces. For these regions, the material normal direction corresponds to the geometric surface normal, and a geometric edge is used to define either the local sheet or fiber direction.

The fiber orientation (as shown in **Figure 6.0.4**) can be visualized by running a datacheck on the mechanical model and examining the output database (ODB) in the Visualization module. Epicardial fiber orientation is shown in red, endocardial fiber orientation is shown in blue, and the average fiber orientation between the epicardium and endocardium is shown in green.

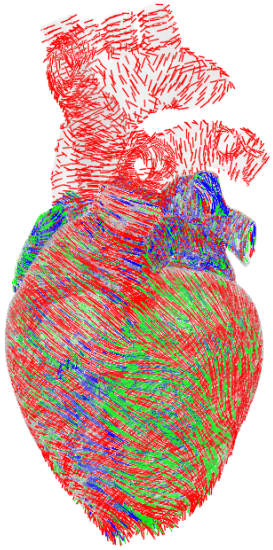

Figure 6.0.4: Fiber orientations of the Heart Model

Should you need to redefine the initial fiber orientations for the atria, ventricles, or any portion thereof, as a result of modifications made to the model geometry (e.g., the creation of a partition in the ventricle that is then remeshed), please consult the **Question & Answer** article entitled "***Redefining the Fiber Orientation in the SIMULIA Living Heart Human Model***" accessible from the Knowledge Base. This article provides instructions to automatically redefine the fiber orientation. You can also override the orientations, in which case you must specify the orientation at the centroid of each element. Since the fiber orientations for the SVC, aortic arch, and pulmonary trunk are defined on the geometry, they will be regenerated automatically upon remeshing; no special user intervention is required. However, you can easily change the fiber angle for these parts, if required.

7 Blood Flow Model

The blood flow model uses a combination of surface-based fluid cavities and fluid exchanges (for more information, refer to Section 11.5 of the **Abaqus Analysis User's Guide [4]**). The circuit shown in **Figure 7.0.1** is a schematic representation of the blood flow model where resistors represent flow resistances and capacitors represent structural compliances.

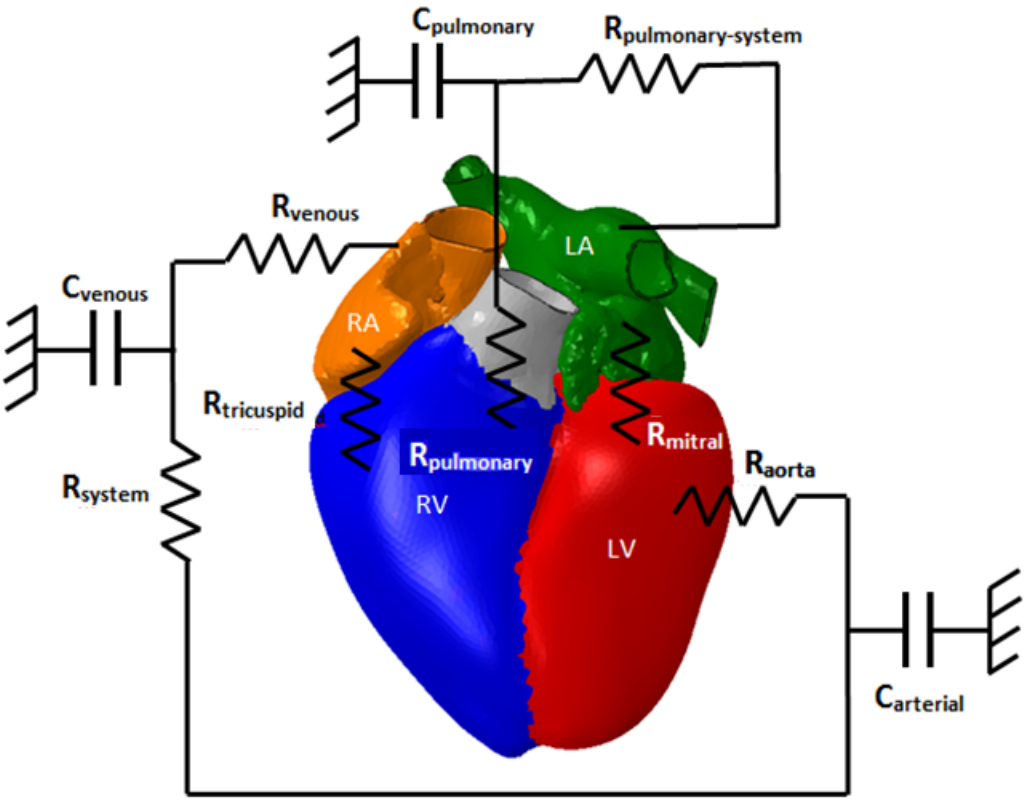

Figure 7.0.1: Schematic representation of the blood flow model

The blood flow model uses the approach described in **Pilla et al. [12]**; however, Pilla et al. use a lumped parameter representation for all components, whereas the Heart Model uses a hybrid approach involving both lumped parameter and 3D representations. In particular, the parameters associated with compliance and contractility of the four heart chambers in Pilla et al. have been replaced by a 3D finite element representation.

The compliance and contractility of the heart within the blood flow model are incorporated into the mechanical simulation through the fluid cavities shown in **Table 7.0.1**.

Table 7.0.1: Hydrostatic fluid cavity definitions

Abaqus/CAE Feature Name	Reference Node Set Name	Surface Name
CAV-AORTA	Aortic_Arch-1.CAV-RP	AORTA-CAV
CAV-LA	L_Atrium-1.CAV-RP	L_Atrium-1.LA-CAV
CAV-LV	LV-RP	LV-CAV
CAV-PULMONARY_TRUNK	Pulmonary_Trunk-1.CAV-RP	Pulmonary_Trunk-1.CAV
CAV-RA	R_Atrium-1.CAV-RP	R_Atrium-1.RA-CAV
CAV-RV	RV-RP	RV-CAV
CAV-SVC	Superior_Vena_Cava-1.CAV-RP	SVC-CAV
CAV-ARTERIAL-COMP	Arterial_Compliance-1.RP	Arterial_Compliance-1.INNER
CAV-PULMONARY-COMP	Pulmonary_Compliance-1.RP	Pulmonary_Compliance-1.INNER
CAV-VENOUS-COMP	Venous_Compliance-1.RP	Venous_Compliance-1.INNER

The last three cavities shown in **Table 7.0.1** are defined as cubic volumes and used to model the compliance of the arterial, venous, and pulmonary circulation systems. Initial dimensions of each cavity are chosen to establish a total blood circulation volume of 5 liters. Each cavity is attached to a grounded spring with a stiffness tuned to provide the appropriate pressure-volume response (i.e., compliance) for that cavity.

Blood flow between the hydrostatic fluid cavities is modeled using the fluid exchange definitions shown in **Table 7.0.2**. Each fluid exchange link possesses a viscous resistance coefficient tuned to obtain atrial and ventricular pressures in accordance with published normal ranges shown in **Table 11.1.1**.

Table 7.0.2: Fluid exchange link definitions

Abaqus/CAE Feature Name	Description	First Chamber	Second Chamber
LINK-ARTERIAL-VENOUS	Extra-cardiac resistance	CAV-ARTERIAL-COMP	CAV-VENOUS-COMP
LINK-VENOUS-RA	Venous resistance	CAV-VENOUS-COMP	CAV-RA
LINK-RA-RV	Tricuspid valve resistance	CAV-RA	CAV-RV
LINK-RV-PULMONARY	Pulmonary valve resistance	CAV-RV	CAV-PULMONARY-COMP
LINK-PULMONARY-LA	Pulmonary resistance	CAV-PULMONARY-COMP	CAV-LA
LINK-LA-LV	Mitral valve resistance	CAV-LA	CAV-LV
LINK-LV-ARTERIAL	Aortic valve resistance	CAV-LV	CAV-ARTERIAL-COMP

Reference values for blood density and bulk modulus are taken from **Mourad and Kargl [13]** as 1.027×10^{-9} tonne/mm^3 and 2.4 MPa, respectively, although the bulk modulus is reduced by a factor of 1000 to increase the stable time increment and thus reduce run time. The reduced stiffness has a negligible effect on the results as the fluid is still significantly stiffer than the muscle in compression.

8 Analysis Procedures

The Heart Model uses a sequentially coupled electrical-mechanical analysis wherein an electrical analysis is conducted first, and the resulting electric potentials are used as the excitation source for a subsequent mechanical analysis. The electrical and mechanical analyses use the same mesh topology. This section describes the analysis workflow in more detail.

8.1 Electrical Analysis

The electrical analysis begins at 70% ventricular diastole in the cardiac cycle (i.e., just prior to atrial systole). The electrical analysis is performed using the **Heat Transfer** procedure in Abaqus/Standard because the governing equations for electrical conduction are equivalent to those used for diffusion heat transfer. Consequently, any references to temperature in the documentation or results files (including ODB output quantity **NT**) actually represent electric potential.

A single analysis step named **BEAT** is defined in the **ELEC** model. The duration of the cardiac cycle is 1 second, but the electrical event (from the onset of depolarization to the end of repolarization across the entire heart) is complete after 500 ms, so for efficiency purposes the electrical simulation is only run for 500 ms. Since the electrical analysis results are used to provide an excitation to the mechanical analysis, the output variable for electrical potential (i.e., temperature **NT**) is specified as field output.

8.1.1 Electrical Boundary Conditions

During the **BEAT** step, an electrical potential pulse (shown in **Figure 8.1.1**) is applied at a node set representing the sinoatrial (SA) node (node set: **R_Atrium-1.SA_NODE**). The electrical waveform is created using the **Smooth Step** amplitude definition and varies from -80 mV to 20 mV over 200 ms as described in **Mulroney and Myers [14]**. The electrical excitation may be changed by editing the Amplitude feature named **SA-NODE** in Abaqus/CAE.

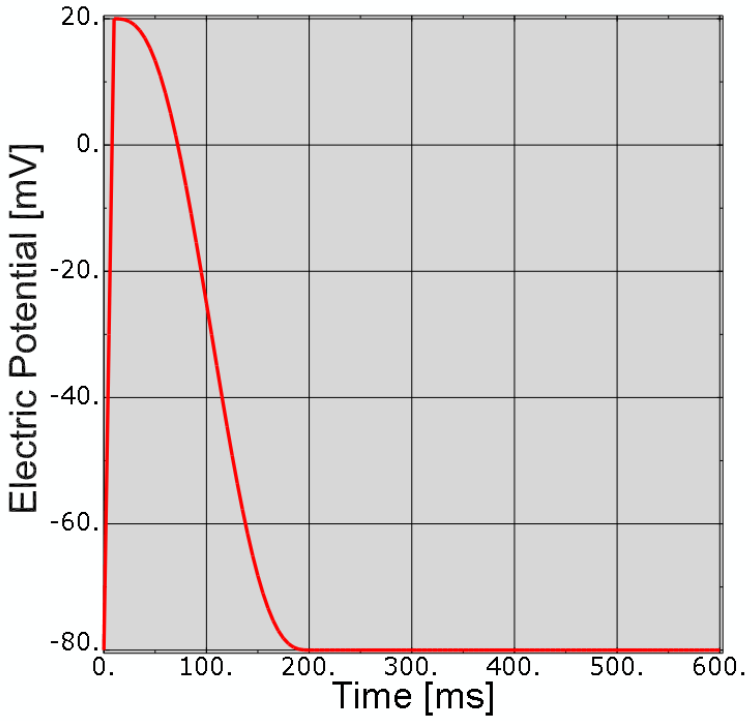

Figure 8.1.1.: The electrical potential at the SA node vs. time

8.2 Mechanical Analysis

The mechanical analysis contains multiple steps as described in **Table 8.2.1** below. Steps 2 and 3 (which together represent one complete cardiac cycle of one second duration) are repeated two additional times (**BEAT2**, **RECOVERY2**, **BEAT3**, **RECOVERY3**) so that three complete cardiac cycles are simulated. After three cardiac cycles virtually all transients in the blood flow model subside and steady state is achieved (see Section 11). To obtain faster turnaround times, you can (i) suppress the second and third beat cycles within Abaqus/CAE if the transients are viewed as insignificant for a particular use case, (ii) increase the amount of mass scaling applied to the model (see Section 8.2.1), or (iii) use the coarse model (See Section 11.7). Any combination of the three methods can be used.

Table 8.2.1: Steps in the mechanical analysis

Step Number	Step Name	Step Time	Description
1	**PRE-LOAD**	0.3 s	Achieve the approximate pre-stressed state of the heart at 70% diastole by linearly ramping up the pressure in the chambers.
2	**BEAT1**	0.5 s	Atrial and ventricular contraction phase of cardiac cycle during which voltages from the electrical analysis (**BEAT**) are applied.
3	**RECOVERY1**	0.5 s	Cardiac relaxation and ventricle filling phase.

In **Figure 8.2.1**, the start and end points for each cardiac cycle is indicated on the Wiggers diagram.

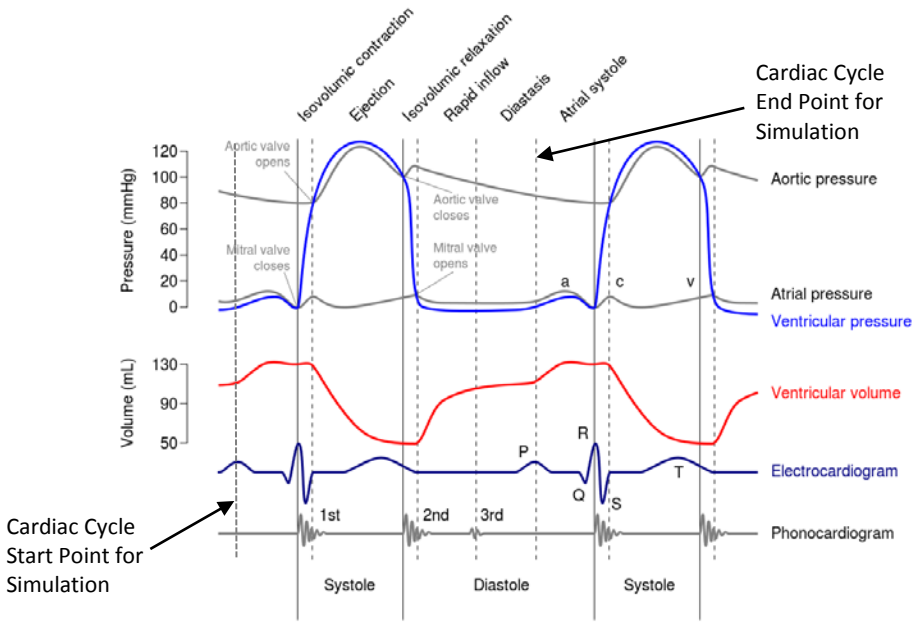

Figure 8.2.1: Wiggers Diagram indicating the start and end points for each cardiac cycle

8.2.1 Mass Scaling

Mass scaling (refer to Section 11.6 of the **Abaqus Analysis User's Guide [4]**) is used throughout the mechanical analysis to reduce the run time. While there are many options for applying mass scaling, in this case, it is set to a value such that the stable time increment remains larger than 2.5e-6 seconds throughout the analysis. The total amount of added mass due to the mass scaling is 0.15% at the start of the analysis; however, this small amount of mass scaling substantially improves performance while having a negligible effect on the results.

8.2.2 Boundary Conditions Applied in All Steps

The heart is constrained via fixed boundary conditions at the cut planes of the aortic arch, pulmonary trunk, and SVC. (node set: **GROUND**). To represent the compliance of the external vasculature, the cut planes are allowed to move relative to fixed reference points by using a **Distributing Coupling** (see **Figure 8.2.2**) with an elastic stiffness such that the maximum motion of the cut planes is less than a few millimeters during the cardiac cycle.

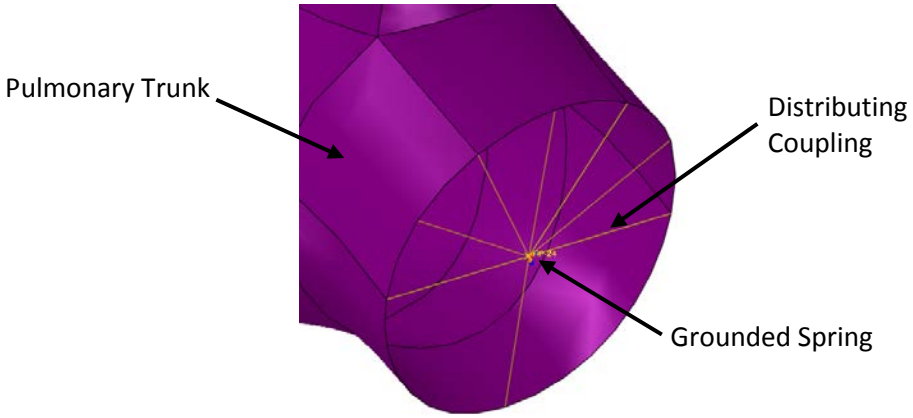

Figure 8.2.2: Boundary conditions at the cut plane of the pulmonary trunk

The volumes of the cavities used to represent the arterial, venous, and pulmonary systems in the blood flow model are dependent on pressure. To account for this dependence, one of the six faces in each cavity is attached to a unidirectional spring while the remaining faces are fixed in all directions. Thus, the node set comprising the faces attached to the springs, **Compliance-AXIAL,** is constrained to move in the X-direction only, whereas the remaining cavity nodes, node set **Compliance-FIXED,** are fully constrained.

8.2.3 Boundary Conditions in the PRE-LOAD Step

In the **PRE-LOAD** step, the pressures within the hydrostatic cavities are ramped up from zero to values cited to be normal at 70% diastole (see **Normal Hemodynamic Parameters [15]**) as shown in **Table 8.2.3**.

Table 8.2.3: Normal Pressures at 70% Diastole

Fluid Cavity	Pressure
CAV-RA	0.0002666 MPa (2 mmHg)
CAV-LA	0.0005333 MPa (4 mmHg)
CAV-RV	0.0002666 MPa (2 mmHg)
CAV-LV	0.0005333 MPa (4 mmHg)
CAV-AORTA	0.01067 MPa (80 mmHg)
CAV-PULMONARY_TRUNK	0.001067 MPa (8 mmHg)
CAV-SVC	0.0002666 MPa (2 mmHg)
CAV-ARTERIAL-COMP	0.010665 MPa (80 mmHg)
CAV-VENOUS-COMP	0.0002666 MPa (2 mmHg)
CAV-PULMONARY-COMP	0.001067 MPa (8 mmHg)

8.2.4 Loads and Boundary Conditions in the Cardiac Cycle Steps (BEAT*n* and RECOVERY*n*)

The pressure boundary conditions described in Section 8.2.3 are removed in step **BEAT1** and all subsequent steps, thus imposing a constant overall blood volume within the circulation system for the remainder of the analysis. The excitation applied to the model (node set: **ALL-NODES**) in every **BEAT*n*** step is the electrical potential history from the electrical analysis. In every **RECOVERY*n*** step, the electrical potential of the entire heart is set to the resting potential (-80 mV). In addition, an electrical potential of -80 mV is applied to the aortic arch, pulmonary trunk, and SVC so that they display the appropriate passive response but do not respond actively.

9 Model Files

The Heart Model is delivered with three Abaqus/CAE databases – **LH-Human-Model.cae**, **LH-Human-Model-Coarse.cae**, and **LH-Human-Model-Fine.cae**. The Heart Model geometry in each database has a different mesh density (see Section 11.7); in all other aspects, the databases are identical. These three separate representations of the Heart Model are intended to (i) allow you to perform a mesh convergence study if needed (see Section 11.7), and (ii) provide you with run-ready representations if you need higher fidelity modeling (-Fine.cae) or faster run times (-Coarse.cae). Each database contains two Abaqus/CAE models – **ELEC** to simulate electrical behavior, and **MECH** to simulate mechanical behavior.

The compressed (**.iso**) file **SIM_Abq_HeartModel.AllOS.1-1.iso** contains the files shown in **Table 9.0.1**. Any file marked with an asterisk (*) is encrypted and can only be used as a ***INCLUDE** file.

Table 9.0.1: Model Files

File Name	Description
README.txt	Readme file that contains model information and legal notices
LH-Human-Model-Coarse.cae LH-Human-Model.cae LH-Human-Model-Fine.cae	The Abaqus/CAE databases containing the less finely meshed ("-Coarse"), medium refinement, and more finely meshed ("-Fine") representations of the model respectively.
Living Heart Human Model Documentation.pdf	Heart Model documentation
nodes_Aortic_Arch-Medium.inp nodes_ASSEMBLY-Medium.inp nodes_L_Atrium-Medium.inp nodes_Pulmonary_Trunk-Medium.inp nodes_R_Atrium-Medium.inp nodes_Superior_Vena_Cava-Medium.inp nodes_Ventricles-Medium.inp	Abaqus input files containing nodal information for the medium refinement representation. Corresponding files for the coarse and fine representations have identical names but with the suffix "-Coarse" and "-Fine" respectively.
L_Atrium-DF-enc.inp* R_Atrium-DF -enc.inp* Ventricles-DF -enc.inp*	Abaqus input files containing the fiber orientations for the atria and ventricles for the medium refinement representation. Corresponding files for the coarse and fine representations have identical names but with the suffix "-Coarse" and "-Fine" respectively.
elec-mat-L_Atrium-enc.inp* elec-mat-Purkinge-enc.inp* elec-mat-R_Atrium-enc.inp* elec-mat-Ventricles-enc.inp*	Abaqus input files containing the constitutive law parameters for the electrical analysis
mech-mat-HYBRID-LA_ACTIVE-enc.inp* mech-mat-HYBRID-LV_ACTIVE-enc.inp* mech-mat-HYBRID-PASSIVE-enc.inp* mech-mat-HYBRID-RA_ACTIVE-enc.inp* mech-mat-HYBRID-RV_ACTIVE-enc.inp*	Abaqus input files containing the constitutive law parameters for the mechanical analysis

10 Submitting the Analyses

All the files needed (including all relevant **`*INCLUDE`** files) for a coupled electrical-structural analysis must be extracted and stored in a single directory from which the analyses are to be run. The electrical analysis must be run at least once before the mechanical analysis. You can (i) submit the simulation directly from Abaqus/CAE, or (ii) write the input file from Abaqus/CAE and submit the analysis via the command line interface. The mechanical analysis must be run in double precision to ensure sufficient accuracy. When submitting the electrical analysis, you must add **`threads=1`** to the execution command (e.g., **`abq6143 job=heart-elec threads=1`**).

DO NOT EDIT THE ABAQUS INPUT FILE. MODIFYING THE MODEL OUTSIDE OF ABAQUS/CAE IS A BREACH OF THE MODEL LICENSE AGREEMENT.

11 Results

The results presented in subsections 11.1 through 11.6 are based on the medium mesh refinement model (**`LH-Human-Model.cae`**). Subsections 11.7 and 11.8 discuss results obtained using the coarse and fine models and other techniques used to improve performance.

11.1 Summary of Simulation Results

A summary of key model results is provided in **Table 11.1.1**. These outputs are clinically meaningful and have been published for normal hearts in reputable sources as referenced. The Heart Model results show good agreement with those presented in the literature.

Table 11.1.1: Key Model Results

Output	Model Result	Published Normal Ranges	Reference # (See Section 14)
L. Ventricle (LV) Ejection Fraction	56%	>50%	[16]
R. Ventricle (RV) Ejection Fraction	49%	40-60%	[15]
Max LV Pressure	136.3 mmHg	100-140 mmHg	[17]
Min LV Pressure	6.8 mmHg	3-12 mmHg	[17]
Max RV Pressure	29.8 mmHg	15-30 mmHg	[17]
Min RV Pressure	0.2 mmHg	2-8 mmHg	[17]
R. Atrium Pressure Range	1.8-6.5 mmHg	2-6 mmHg	[15]
L. Atrium Pressure Range	8.7-24.5 mmHg	4-12 mmHg	[15]
Maximum LV Apex-Base Shortening	8.6 mm (see Section 11.3)	11.2 ± 3.8 mm	[18]
Apical Twist	10.9° (see Section 11.4)	No Result[1]	--

[1] Numerous references for apical twist were reviewed and in nearly every one the twist is measured in a different manner using image data and as such a wide range of twist has been reported in the literature.

11.2 Cardiac Cycle Steady State Response

Figure 11.2-1 illustrates the transient behavior of the pressure-volume (PV) loop of the left ventricle (LV). The PV loop (and, hence, the ejection fraction) is very close to steady state after three cycles, although the figures below were generated using five cardiac cycles to confirm this result. **Figure 11.2-2** shows the fiber strain on the wall of the LV (node set: **`LOC-8_L_VENTRICLE`**).

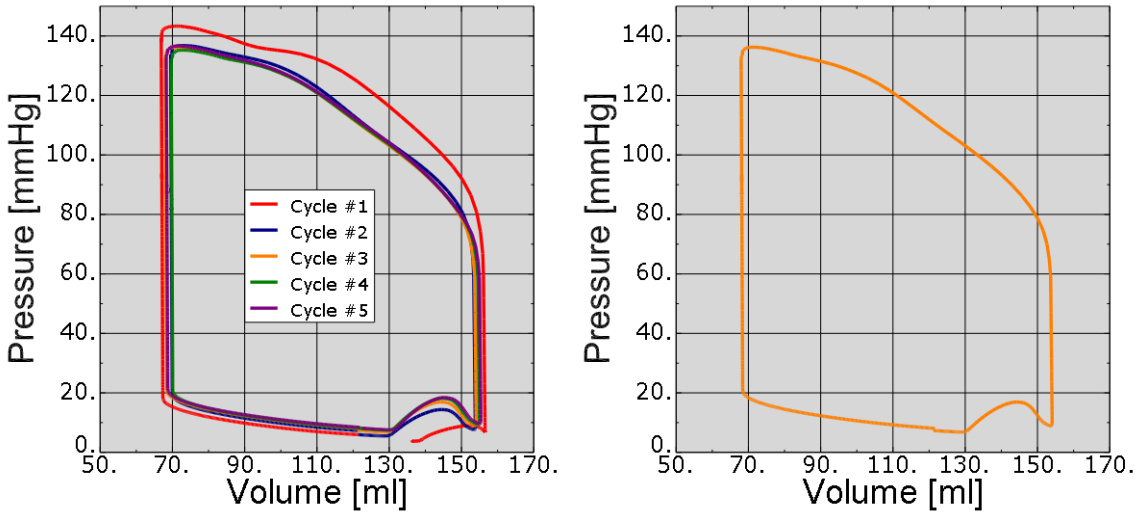

Figure 11.2.1: Pressure-Volume Loops of the LV for Cardiac Cycles 1-5 (left) and Cycle 3 only (right)

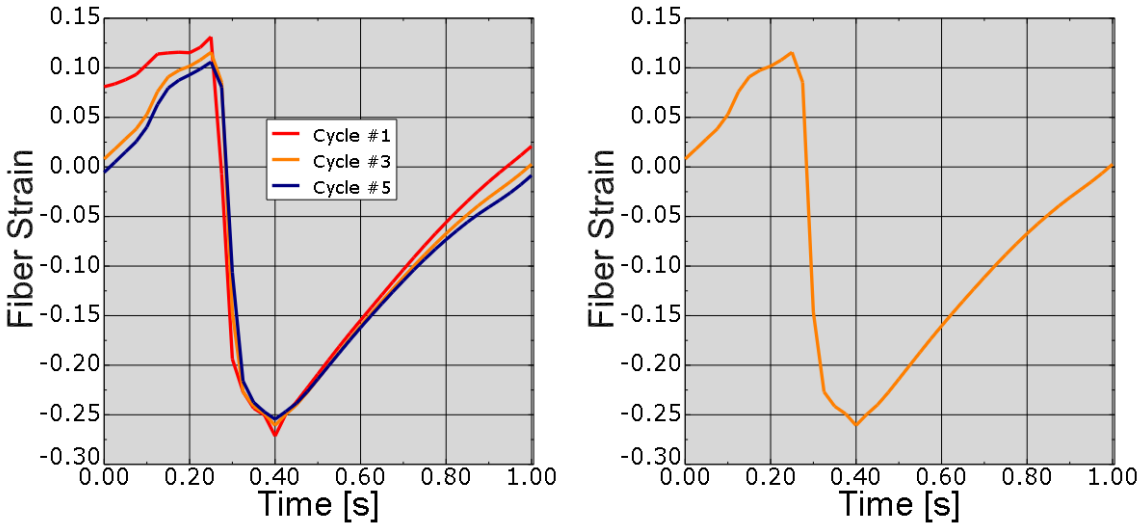

Figure 11.2.2: LV Wall Fiber Strain for Cardiac Cycles 1, 3 and 5 (left) and Cycle 3 only (right)

11.3 Apex-to-Base Shortening

The apex-to-base shortening is measured by attaching an axial connector element (element set: **APEX-TO-BASE**) to the left ventricular apex and center of the mitral valves planar surface (the base). The history output request **CU1** (relative displacement of the axial connector) is used to monitor the apex-to-base shortening throughout the simulation.

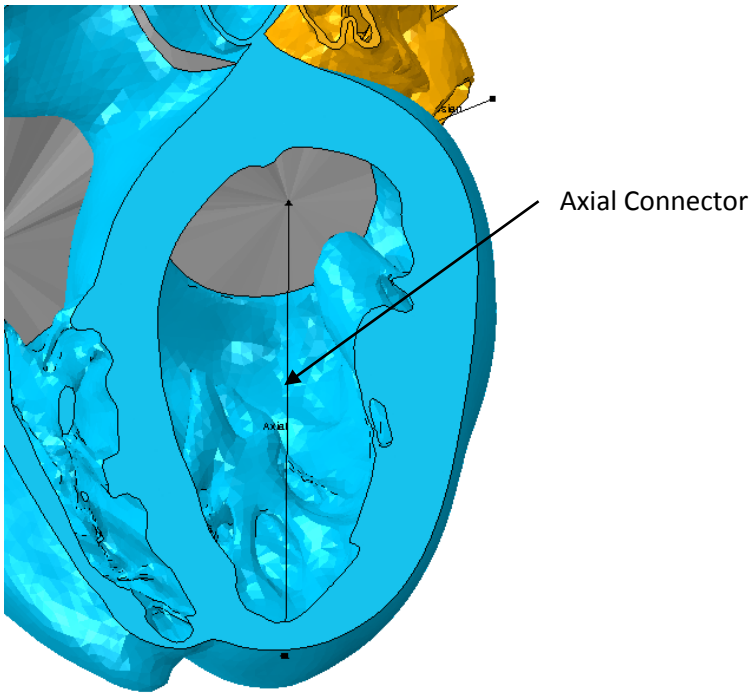

Figure 11.3.1: Axial Connector used to measure the Apex-to-Base shortening

Figure 11.3.2 illustrates the apex-to-base shortening and is very close to steady state after two cycles.

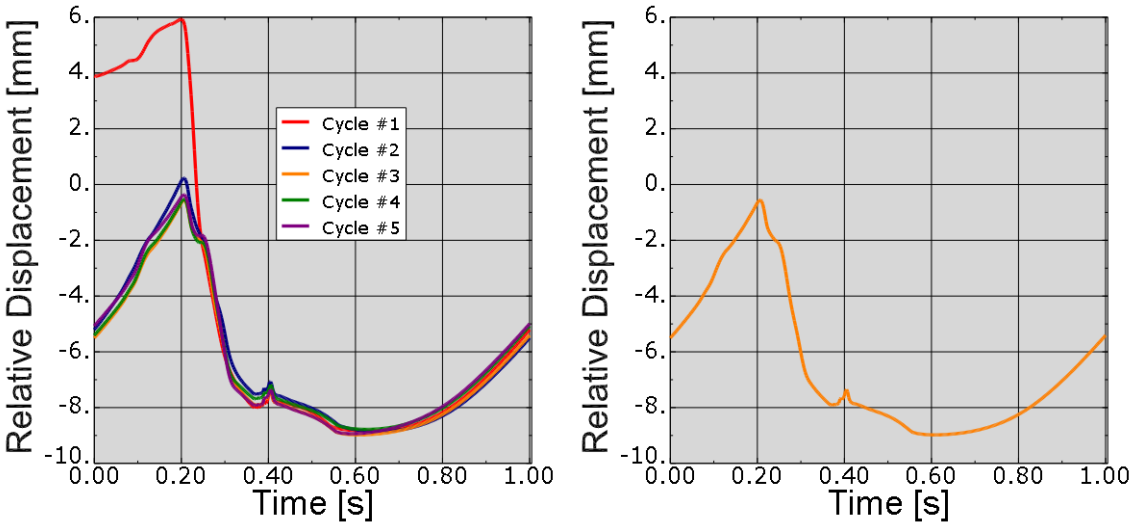

Figure 11.3.2: Apex-to-Base shortening for the Cardiac Cycles 1-5 (left) and Cycle 3 only (right)

11.4 Apical Twist

The apical twist is measured by tracking the average rotation of 4 nodes on the left ventricle's apex. The average motion is tracked by defining a distributing coupling with nodes **`Ventricles-1.1179`**, **`Ventricles-1.7323`**, **`Ventricles-1.7212`**, and **`Ventricles-1.7025`** as the coupled nodes and assembly node 28 as the control node (See **Figure 11.4.1**). The control node is connected to ground through a zero stiffness Cardan connector. A history output request **CUR1** for the connector (element set: **`ROTATION-MEASURE`**) is used to monitor the twist.

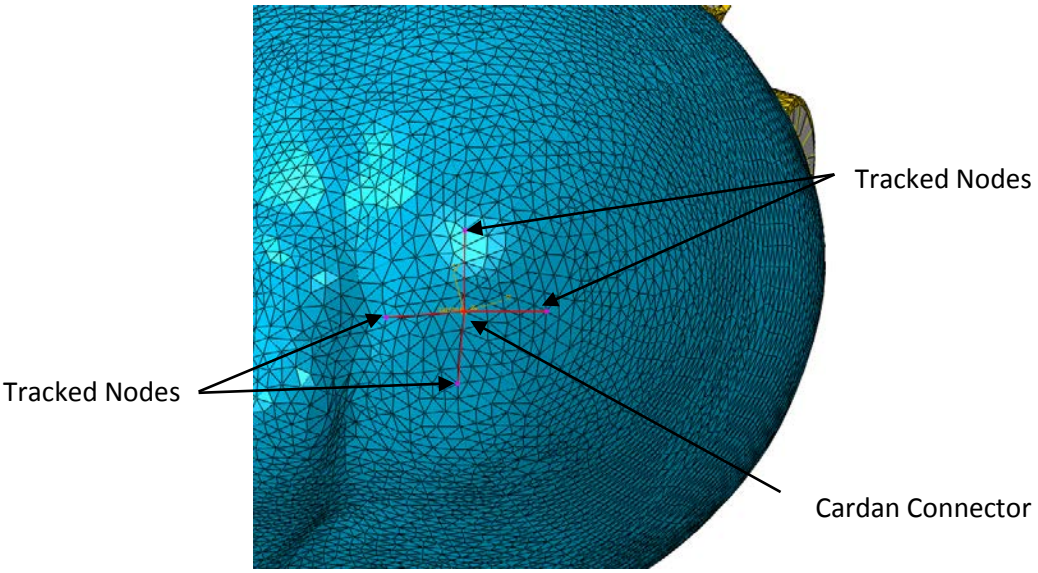

Figure 11.4.1: Methodology used to measure Left Ventricle Apical Twist

11.5 Electrical Potential

The electrical potential as a function of time is shown in **Figure 11.5.1** at select times during the analysis. The activation times predicted by the model compare well with estimated activation times for normal heart function (See Conduction Systems Tutorial [9]) in **Figure 11.5.2**.

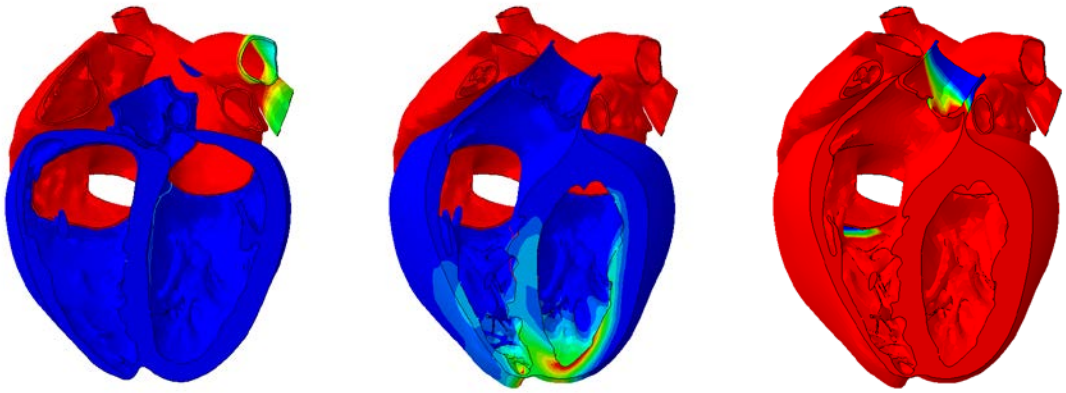

Figure 11.5.1: Electric Potential in the Heart (at 90 ms, 180 ms, 230 ms) – Maximum (red): 20mV; Minimum (blue): -80mV

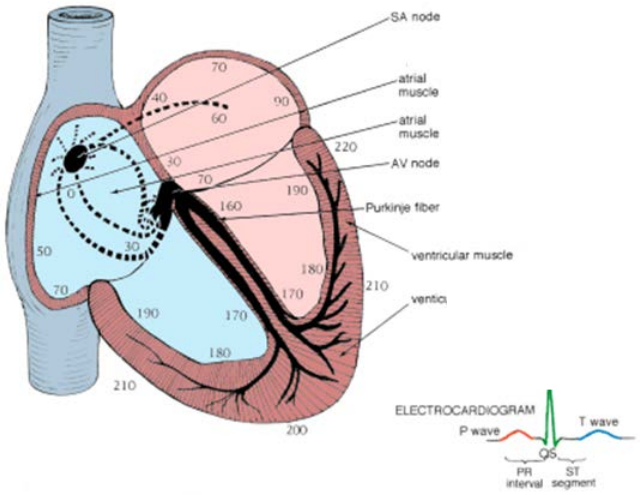

Figure 11.5.2: Plot of Normal Activation Times throughout the Heart (from Conduction Systems Tutorial [9])

11.6 Mechanical Deformation

A primary output from the mechanical analysis is heart deformation as a function of time and is shown in **Figures 11.6.1 through 11.6.3** at select times during the analysis.

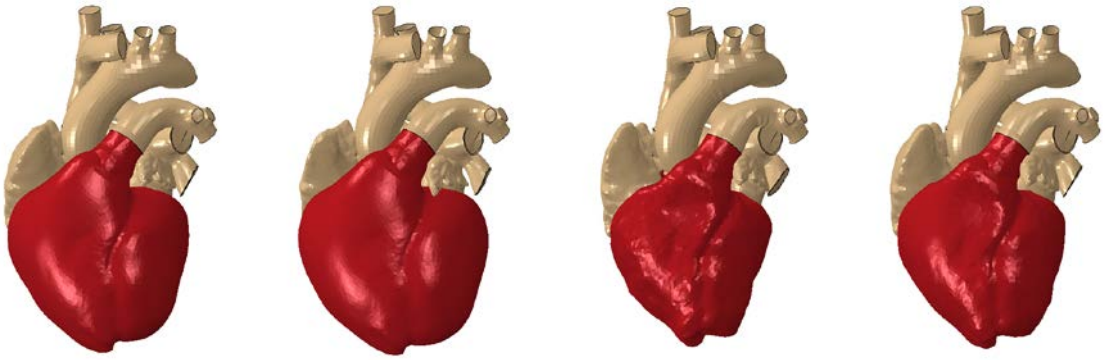

Figure 11.6.1: Deformation of the Heart at 0.0 s, 0.2 s, 0.5 s, 0.7 s of the 3rd cardiac cycle

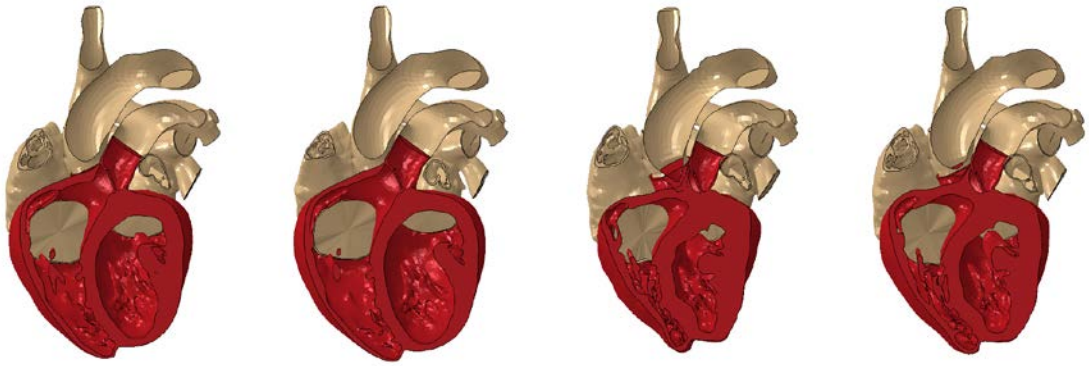

Figure 11.6.2: Deformation at Vertical Cut of the Heart at 0.0 s, 0.2 s, 0.5 s, 0.7 s of the 3rd cardiac cycle

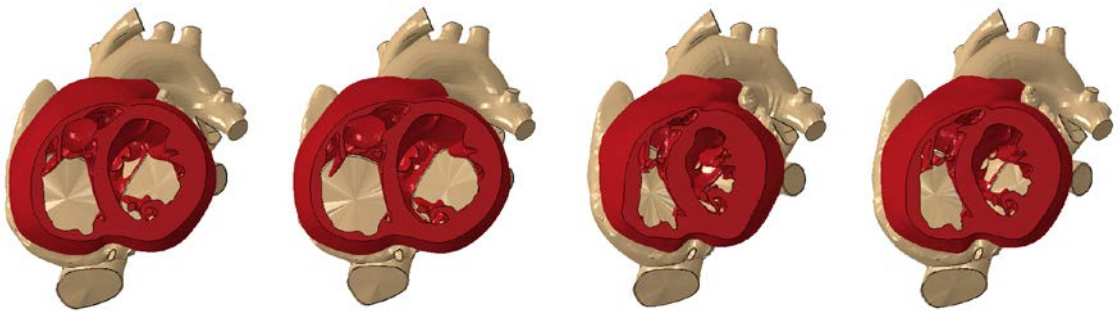

Figure 11.6.3: Deformation at Horizontal Cut of the Heart at 0.0 s, 0.2 s, 0.5 s, 0.7 s of the 3rd cardiac cycle

11.7 Mesh Convergence

The coarse, medium, and fine representations of the model and their model sizes are shown in **Figure 11.7.1** and **Table 11.7.1**, respectively. Unless otherwise noted, the medium representation has been used to generate all the images, tables, and results data throughout this document, as it provides a balance of solution accuracy and performance.

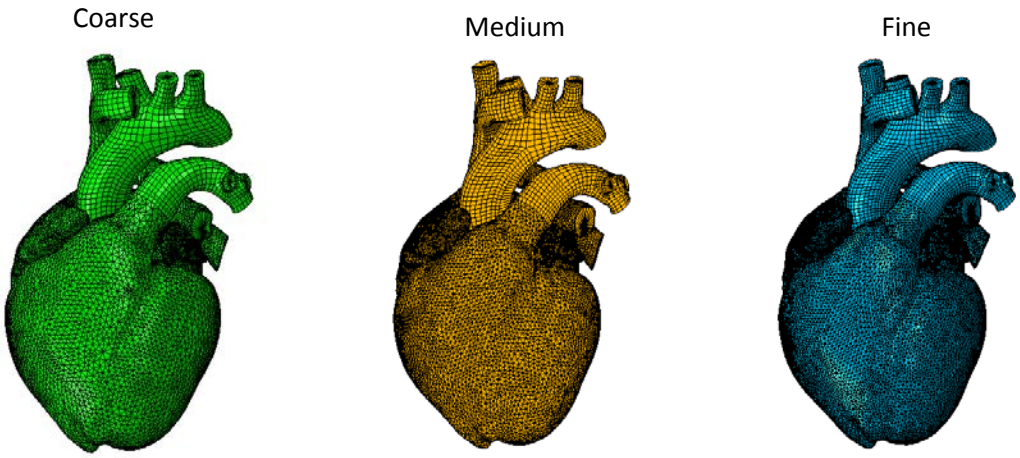

Figure 11.7.1: The Heart Model Mesh Refinement representations

Table 11.7.1: Total Number of Nodes, Elements and DOF for Each Heart Model Representation

Simulation	Representation	Total Number of Nodes	Total Number of Elements	Total Number of DOF
Electrical	Coarse	67299	263005	67299
	Medium	92549	371101	94549
	Fine	132288	547558	132288
Mechanical	Coarse	71389	266381	220707
	Medium	97950	375675	302977
	Fine	139756	554031	432736

11.7.1 Electrical Convergence

Mesh convergence for the electrical analysis is examined at eight points (highlighted in red in **Figure 11.7.1.1**) because these are typical locations at which pacemaker leads are placed.

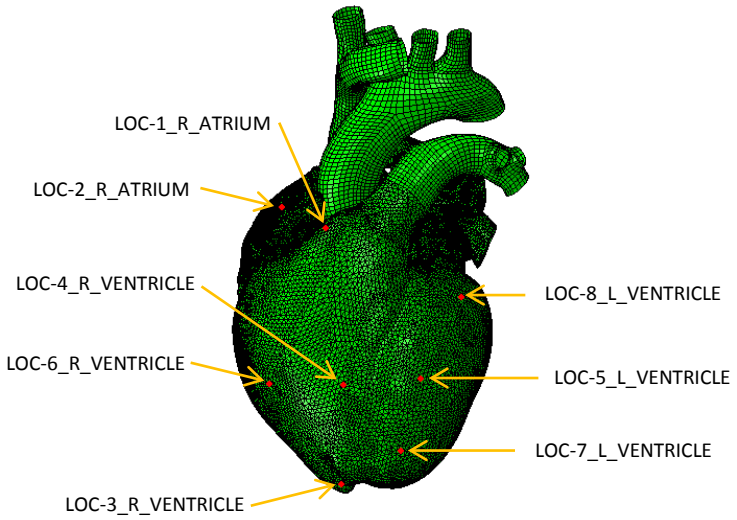

Figure 11.7.1.1: Electric Potential Mesh Convergence comparison locations

The metric used to assess convergence is the simulation time at which the tissue reaches an electrical potential magnitude of -40 mV ("the activation time"). A summary of these results can be found in **Table 11.7.1.1**.

Table 11.7.1.1: Summary Activation Times for Mesh Convergence Study

Node Set	Refinement		
	Coarse	Medium	Fine
LOC-1_R_ATRIUM	40.3 ms	40.4 ms	40.2 ms
LOC-2_R_ATRIUM	48.3 ms	48.3 ms	48.1 ms
LOC-3_R_VENTRICLE	188.6 ms	194.8 ms	208.2 ms
LOC-4_R_VENTRICLE	196.5 ms	203.6 ms	214.9 ms
LOC-5_L_VENTRICLE	220.2 ms	226.5 ms	239.5 ms
LOC-6_R_VENTRICLE	200.0 ms	206.8 ms	220.2 ms
LOC-7_L_VENTRICLE	175.7 ms	182.4 ms	193.4 ms
LOC-8_L_VENTRICLE	215.5 ms	221.8 ms	233.7 ms

The time histories of the electrical potential over the entire **BEAT** step for three of these locations (LOC-2_R_ATRIUM, LOC-3_R_VENTRICLE, and LOC-8_L_VENTRICLE) are illustrated in **Figure 11.7.1.2**.

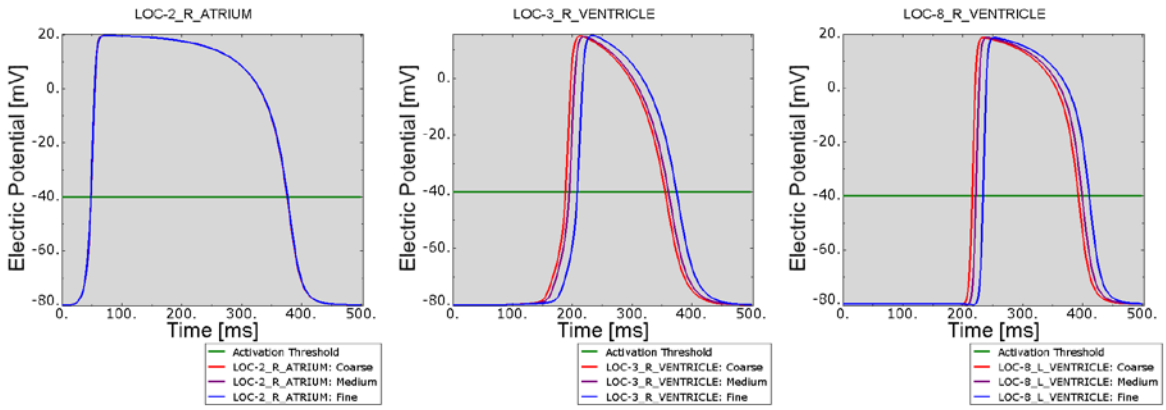

Figure 11.7.1.2: Time Histories of Electrical Potential for three selected points

Temporal convergence was also assessed by running simulations in which the time increment was controlled by specifying a limit for the maximum (absolute value) allowable change in electrical potential at any node in the model during any single time increment. Maximum electrical potential changes of 20, 10, and 5 mV were assessed at each of the locations. The results indicated that the solution is not significantly affected by time increment size and as such the electrical model uses a change in electrical potential of 20 mV to control the time increment size.

11.7.2 Mechanical Convergence

The metrics used to assess the convergence of the mechanical analysis are the same clinical meaningful outputs that are reported in **Table 11.1.1**. A summary of these results is shown in **Table 11.7.2.1**.

Table 11.7.2.1: Summary of Results for Mesh Convergence Study

Output	Refinement		
	Coarse	Medium	Fine
L. Ventricle (LV) Ejection Fraction	56%	56%	56%
R. Ventricle (RV) Ejection Fraction	49%	49%	48%
Max LV Pressure	135.4 mmHg	136.3 mmHg	137.6 mmHg
Min LV Pressure	6.6 mmHg	6.8 mmHg	7.0 mmHg
Max RV Pressure	29.8 mmHg	29.8 mmHg	30.1 mmHg
Min RV Pressure	0.0 mmHg	0.2 mmHg	0.5 mmHg
R. Atrium Pressure Range	1.0-6.4 mmHg	1.8-6.5 mmHg	1.8-6.6 mmHg
L. Atrium Pressure Range	8.4-23.3 mmHg	8.7-24.5 mmHg	9.0-25.9 mmHg
Maximum LV Apex-Base Shortening	8.5 mm	8.6 mm	8.5 mm

11.8 Run-Time Performance

The results of a run-time scaling study for the mechanical model are shown in **Table 11.8.1** and graphically in **Figure 11.8.1**, respectively. The run times shown are for analyses in which three beat cycles are conducted. These analyses were conducted on a Linux 64 cluster, containing Intel Xenon E5-2680 v2 (Ivy Bridge) chip sets, with a 10 Gb/s interconnect, each with 16 cores. The compute times shown in the table are representative only since hardware and system configuration can have a significant effect on performance.

The electrical model was run on 16 CPUs using the same system configuration as the mechanical model. Run times for the coarse, medium, and fine models were 46 minutes, 64 minutes, and 105 minutes respectively. A scaling study for the electrical model was not performed since the relatively short run time did not warrant such a study.

Table 11.8.1: Run-Time Performance Results Summary for Mechanical Model

Representation	Number of CPUs	Wall Clock Run Time [hrs.]
Coarse	8	44.8
	16	17.3
	32	11.2
	64	6.2
Medium	8	64.1
	16	35.0
	32	17.9
	64	8.8
Fine	8	101.4
	16	42.6
	32	25.6
	64	13.7

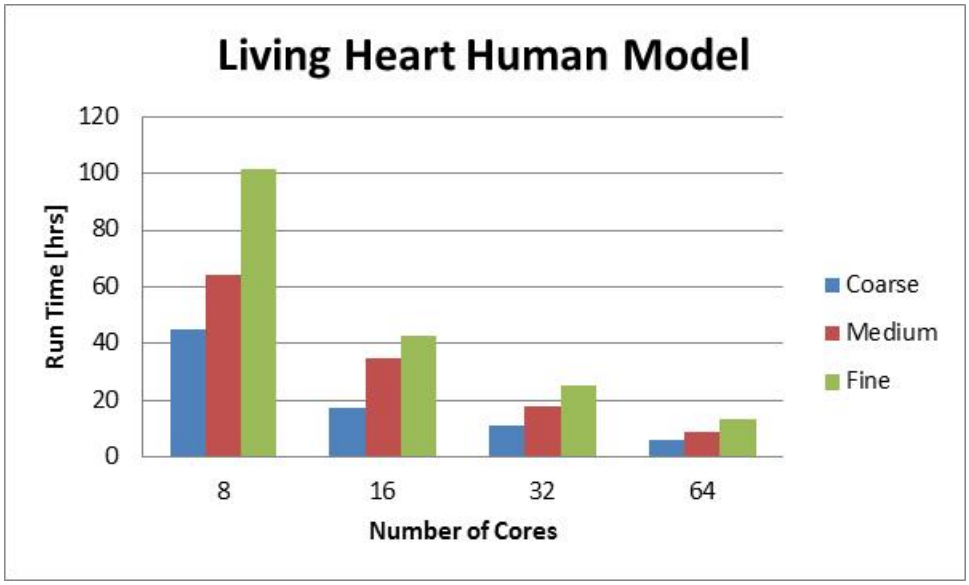

Figure 11.8.1: Run-Time Performance Results Summary for Mechanical Model

12 Verification and Validation

SIMULIA utilizes ISO 9001:2008 certified processes for verification and benchmarking for the development of its simulation software applications. See the **Abaqus Verification and Benchmarks Guides [20] & [21]** for published problem suites. These same processes for verification and validation were applied to the Heart Model.

12.1 Verification

Verification is a process to establish and confirm that the results from a simulation model reproduce those from an associated mathematical model. Verification includes unit testing, convergence studies, and computational platform testing.

SIMULIA has developed a suite of four problems that verify the implementation of the constitutive equations for the electrical and mechanical passive and active response of the cardiac tissue. These problems are available upon request.

12.2 Validation

Validation encompasses quality assurance and model correctness activities surrounding the development of a simulation model and the custom software components it utilizes or contains. Validation activities specific to the Heart Model are described below.

12.2.1 Model Validation

Model Validation encompasses comparison against generally expected behavior (e.g., measured against published and generally accepted metrics like pressure-volume loops, ECG traces, overall motion, etc.). The simulation results presented in **Table 11.1.1** represent the current status of the Heart Model validation.

12.2.2 Intended Use Validation

Intended Use Validation is a part of the overall validation for a procedure or treatment that will often involve specific medical devices. Intended use validation is confirmation by the provision and examination of objective evidence that the model is predictive for each specific intended use. A conclusion that the model is validated for its intended use is highly dependent upon comprehensive testing, inspections, data analyses, and simulation result comparisons against measurement data.

SIMULIA has not performed any Intended Use Validation on the Heart Model and recognizes that it will not be suitable for all applications.

13 References

- [1] Kotikanyadanam, M., Göktepe, S., Kuhl, E. "Computational modeling of electrocardiograms: A finite element approach toward cardiac excitation." *International Journal for Numerical Methods in Biomedical Engineering*. 2010 (26): 524-533.
- [2] Baillargeon, B., Costa, I., Leach, J.R., Lee, L.C., Genet, M., Toutain, A., Wenk, J.F., Rausch, M.K., Rebelo, N., Acevedo-Bolton, G., Kuhl, E., Navia, J.L., Guccione, J.M. "Human cardiac function simulator for the optimal design of a novel annulopasty ring with a sub-valvular element for correction of ischemic mitral regurgitation." *Cardiovascular Engineering and Technology*. Submitted.
- [3] Prot, V., Haaverstad, R., and Skallerud, B. "Finite element analysis of the mitral apparatus: annulus shape effect and chordal force distribution." *Biomech Model Mechanobiol* (2009) 8: 43-55.
- [4] Abaqus 6.14 Analysis User's Guide, 2014. *Dassault Systèmes Simulia Corporation.*
- [5] Holzapfel, G.A., and Ogden, R.W. "Constitutive modelling of passive myocardium: a structurally based framework for material characterization." *Philosophical Transactions of the Royal Society A* (2009) 367: 3445-3475.
- [6] Genet, M., Lee, L.C., Kuhl, E., and Guccione J. *Abaqus/Standard-Based Quantification of Human Cardiac Mechanical Properties*. SIMULIA Customer Community Conference. Providence, Rhode Island. May 2014.
- [7] Walker, J.C., Ratcliffe, M.B., Zhang, P., Wallace, A.W., Fata, B., Hsu, E., Saloner, D., and Guccione, J. "MRI-based finite-element analysis of left ventricular aneurysm." *Am U Physiol Heart Circ Physiol* (2005) 289: H692-H700.
- [8] Hurtado, D., and Kuhl, E. "Computational modeling of electrocardiograms: repolarization and T-wave polarity in the human heart." *Computer Methods in Biomechanics and Biomedical Engineering* (2012): 1-11.
- [9] *Conduction System Tutorial – Gap Junctions.* http://www.vhlab.umn.edu/atlas/conduction-system-tutorial/gap-junctions.shtml. (http://dx.doi.org/10.1016/j.euromechsol.2014.04.001).
- [10] Streeter, D.D., Spotnitz, H.M., Patel, D.P., Hoss, J., Sonnenblick, E.H. "Fiber Orientation in the Canine Left Ventricle during Diastole and Systole." *Circulation Research*. 1969 (24): 339-347.
- [11] *euHeart. Final Project Report*. 2007. http://www.euheart.eu/fileadmin/system/euheart/documents/euHeart_report.pdf.
- [12] Pilla, J.J., Gorman, J.H., Gorman, R.C. "Theoretic Impact of Infarct Compliance on Left Ventricle Function." *Ann Thorac Surg*. 2009. 87(3): 803-810.
- [13] Mourad, P.D. and Kargl, S.G. *Acoustic Properties of Fluid-Saturated Blood Clots.* Technical Report. University of Washington. APL-UW TR 2003 (2003):pg. 7.
- [14] Mulroney, S. and Myers, A.K. *Netter's Essential Physiology*. 2009. Elsevier.
- [15] *Normal Hemodynamic Parameters – Edwards Lifesciences*. http://ht.edwards.com/scin/edwards/fr/sitecollectionimages/edwards/products/presep/ar04313hemodynpocketcard.pdf.
- [16] Phibbs, B. *The Human Heart: A Basic Guide to Heart Disease – Second Edition*. Lippincott Williams & Wilkins. 2007.
- [17] Klingensmith, M.E., Chen, L.E., Glasgow, S.C., Goers, T.A., Melby, S.J. *The Washington Manual of Surgery – Fifth Edition*. Lippincott Williams & Wilkins. 2005.
- [18] Rogers et. al. "Quantification of and correction for left ventricular systolic long-axis shortening by magnetic resonance tissue tagging and slice isolation." *Circulation* (1991) 84:2 721-731.
- [19] Marcelli, E., Cercenelli, L., Musaico, M., Bagnoli, P. "Assessment of Cardiac Rotation by Means of Gyroscopic Sensors." *Computers in Cardiology*. 2008 (35): 389-392.
- [20] Abaqus 6.14 Benchmarks Guide, 2014. *Dassault Systèmes Simulia Corporation.*
- [21] Abaqus 6.14 Verification Guide, 2014. *Dassault Systèmes Simulia Corporation.*